2021 43rd Annual International Conference of the
IEEE Engineering in Medicine & Biology Society (EMBC)
Oct 31 - Nov 4, 2021. Virtual Conference

Application of Stochastic Dosimetry for assessing the Human RF-EMF Exposure in a 5G indoor Scenario

M. Bonato, L. Dossi, E. Chiaramello, M. Benini, S. Gallucci, S. Fiocchi, G. Tognola and M. Parazzini, *Member, IEEE*

***Abstract*— In recent years the introduction of 5G networks is causing a drastically change of human exposure levels in the radio frequency range. The aim of this paper is on expanding the knowledge on this issue, assessing the exposure levels for a particular case of indoor 5G scenario, where the presence of an Access Point (AP) was simulated. Coupling the traditional deterministic computational method with an innovative stochastic approach, called Polynomial Chaos Kriging, allowed to evaluate the exposure variability of an user considering the 3D beamforming capability of the antenna. The exposure levels, expressed in terms of specific absorption rate (SAR) in specific tissues, showed low values compared to ICNIRP guidelines.**

I. Introduction

In the recent years one of the major technological innovation is the deployment of 5th generation (5G) mobile networks, which will involve an expansion and an evolution respect to the existing 4th generation (4G) networks. 5G networks are indeed designed to satisfy the users' new needs such as an increase of number of connected devices, data rate and a low transmission latency, characterizing the future with the reality of smart cities, homes, societies and Internet of things (IoT) world [1]. To achieve these ambitious requirements, in the last release of the standardization group 3rd Generation Partnership Program (3GPP) it was underlined that one of key point in 5G networks is the use of the millimeter wave (mmWave) bands (30 - 300 GHz), to make available very large channel bandwidths. However, the very high path loss that the signal experiences at these frequencies need to be counterbalanced by the adoption of innovative technologies, such as dense micro cells' deployment, massive multiple-input-multiple-output (MIMO) systems and three-dimensional beamforming (3DBF) capability for the antennas, to obtain high focalized beams only in the desired direction [2-4].

Although all the benefits that 5G networks are nowadays bringing, these innovations will also imply a drastically change on the RF-EMF exposure levels of the population, causing public concern [5]. This issue was also pointed out lately by the IEEE Committee on Man and Radiation (COMAR), where it was highlighted the need of more high-quality research in the RF range exposure scenario, primarily because the population has not previously been exposed massively to mmWave spectrum [6].

In literature there are now studies on the human exposure assessment considering the deployments of 5G networks, some of them evaluating the exposure in downlink and uplink scenarios but limiting the exposure assessment only on a few configurations [7-9], others facing the exposure variability of the scenario by using ray tracing and statistical techniques [10-12]. Indeed, one of the major challenges is still the assessment of the levels of exposure taking into account the variability and heterogeneity that characterize 5G exposure scenarios, without investing enormous computational costs.

The present work fits in this context and is focused on a specific case of indoor environment, where the presence of a 5G Access Point (AP) was simulated. To not limit the analysis on only some worst-cases exposure scenario, both deterministic and stochastic dosimetry were jointly applied. In this way, it was possible to consider the exposure variability due to 3D beamforming capability of the AP. Stochastic dosimetry is a successful methodology that was applied before at LF (low frequency) and RF ranges, proving its validity in deal with highly variable and heterogeneous scenarios [13,14]. In this case, the stochastic dosimetry approach, called Polynomial Chaos Kriging, allowed to consider up to 1000 different beamforming patterns of the antenna, with low computational costs. The exposure levels were evaluated in terms of specific absorption rate (SAR), following the ICNIRP guidelines [15]. Details of the work are described in the following paragraphs.

II. Materials and Methods

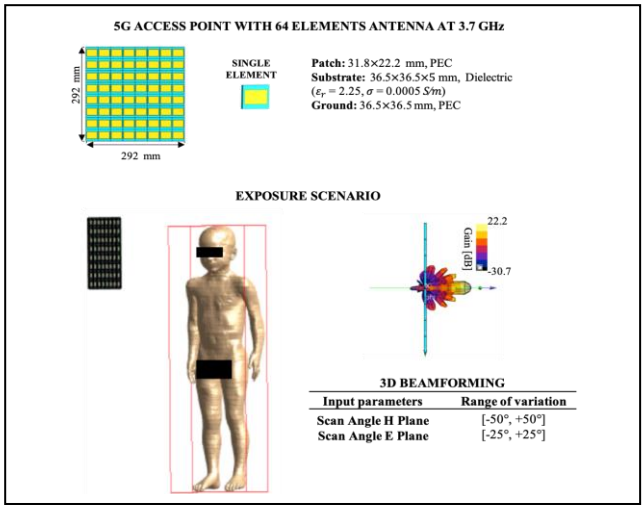

Figure 1. In the upper part, the details of the 5G AP antenna model, in the lower part, the exposure scenario with Roberta model and the ranges of the two input scan angles.

M. B., L. D., E. C., M. B., S. G., S. F., G. T., M. P. are with the Institute of Electronics, Computer and Telecommunication Engineering (IEIIT), CNR, Milano 20133, Italy (corresponding author: marta.bonato@ieiit.cnr.it).

M. B., M. B., S. G. are also with the Department of Electronics, Information and Bioengineering (DEIB), Politecnico di Milano, Milano 20133, Italy.

Figure 1 shows the exposure scenario and the antenna model. The AP was modelled considering the innovation technologies of 5G networks, i.e. new frequency ranges, a dense microcell deployment and beamforming capability, resulting in 64 elements antenna with 3DBF capability, working at 3.7 GHz. In detail, each element of the antenna is composed by a patch antenna, where the patch and ground layers are modelled as PEC material and the substrate layer is modelled as dielectric (properties: ε_r= 2.25 and σ = 0.0005 S/m, data from [10]). Furthermore, each element of the AP was excited with a Gaussian signal for a total input power of 100 mW, in line with the maximum allowed input power values specified in the 3rd Generation Partnership Project [16]. At last, the 3DBF capability is regulated by the two scan angles of the direction of the main beam in the space. The first scan angle regulates the beamforming in the H-plane (horizontal plane) with a range of variation between [-50°; +50°], whereas the second one regards the beamforming direction in the E-plane (elevation plane), varying between [-25°; +25°]. To assess the exposure levels, the child Roberta model (age = 5 years old, height = 1.1 m, mass = 17.6 kg and BMI = 14.8 kg/m) from Virtual Classroom was used [17]. The model was placed in a lateral position 50 cm far away from the AP, i.e. in the worst exposure conditions found in [18]. The exposure was evaluated in terms of SAR mediated on whole tissues or mediated on 10g.

The procedure for combining successfully deterministic dosimetry with the innovative stochastic approach, in order to evaluate the exposure variability caused by the variability of the 3D beamforming pattern, is explained in details in the following paragraphs. In particular in "A. Design of the Experiment" the deterministic dosimetry has been used for finding a set of N experimental observations regarding the variable of interest, necessary to build the surrogate model. In "B. Polynomial Chaos Kriging and Surrogate Model Validation" the surrogate models were obtained with stochastic dosimetry and were validated thanks to a cross validation technique, in order to define the minimum number N of simulations necessary to achieve an acceptable error. Lastly, in "C. Analysis of the Exposure", the surrogate models were useful to evaluate the variability of exposure considering the beamforming capability of the AP.

A. Design of the Experiment

The probability functions of the two different scan angles were supposed uniformly distributed, meaning that each beamforming pattern has the same probability to appear. Furthermore, the Latin Hypercube sampling (LHS) method was used on the probability density functions of the two scan angles to generate the input coordinates [19].

The Sim4life platform (ZMT Zurich Med Tech AG, Zurich, Switzerland, www.zurichmedtech.com) was involved to conduct the deterministic dosimetry simulations based on the set of input coordinates, using the finite-difference time-domain (FDTD) solver. The computational simulations included the 5G AP and the entire model of Roberta, which was discretized with a non-uniform grid with a maximum step of 0.9 mm. The dielectric properties of Roberta's tissues were chosen according to the literature [20, 21], considering the working frequency of 3.7 GHz. At last, the domain boundaries were assumed perfectly matched layer (PML) absorbing conditions.

The exposure assessment was conducted evaluating the specific absorption rate (SAR) in some specific tissues of the model. Precisely, the SAR averaged on tissue mass was evaluated for the whole body, the whole head and the whole brain, where the following tissues were included in the brain: brain grey matter, brain white matter, hypothalamus, hippocampus, hypophysis, midbrain, medulla oblongata, pineal body, pons, and thalamus. Additionally, the SAR averaged on 10 g was assessed for the skin, the brain grey matter, and the cerebellum.

The deterministic dosimetry provided the results that were used to implement the surrogate models using the Polynomial Chaos Kriging method, as described in the following paragraph.

B. Polynomial Chaos Kriging and Surrogate Model Validation

The stochastic approach chosen for this work is called Polynomial Chaos Kriging (PC-Kriging) technique. PC-Kriging is a novel metamodeling technique, never applied before in the framework of 5G exposure assessment, that consists in combining the advantages of Kriging (Gaussian process modelling) with those of Polynomial Chaos Expansions (PCE) [22, 23]. In detail, the PC-Kriging is a universal kriging model, whose trend is obtained by a sparse set of orthogonal polynomials. The PC-Kriging can be expressed by the following form:

$$\hat{Y}^{PCK} = \hat{M}^{PCK}(\boldsymbol{x}) = \sum_{j=1}^{p} \alpha_j \psi_j(\boldsymbol{X}) + Z(\boldsymbol{x}), \quad (1)$$

where the first term $\sum_{j=1}^{p} \alpha_j \psi_j(\boldsymbol{X})$ individuates the model trend, using the PCE solution, and the second term Z(x) represents the calibration term, for describing the stationary Gaussian process with zero mean and stationary autocovariance, in the form:

$$\mathrm{E}[Z(\boldsymbol{x}), Z(\boldsymbol{x}')] = \sigma^2 R(\boldsymbol{x} - \boldsymbol{x}', \boldsymbol{\theta}), \quad (2)$$

where σ^2 is the (constant) variance of the Gaussian process, and R is its stationary autocorrelation, depending on the difference between two sample points $(\boldsymbol{x} - \boldsymbol{x}')$ and its hyperparameters $\boldsymbol{\theta}$.

It is clear that two different steps are necessary to obtain the surrogate models. The first one is the determination of the orthogonal polynomials and of the unknow coefficient α_j and the second one is the calibration of Kriging model, calculating the variance σ^2 and the hyperparameters θ of the autocorrelation function R.

Furthermore, there are various techniques to jointly optimize the two parts and here it was chosen to use the optimal PC-Kriging (OPCK) to minimize the leave-one-out error. Regarding the first step, the Legendre polynomials up to the fourth order were selected as polynomial basis, considering that the probabilistic input functions were uniformly distributed and the unknow coefficients α_j were evaluated by least angle regression selection (LARS) algorithm [24]. For the second step, the autocorrelation function R was estimated using Matérn correlation function and its hyperparameters σ^2 and $\boldsymbol{\theta}$ were calculated by cross-validation estimation and

covariance matrix adaptation-evolution strategy (CMA-ES) [25].

The procedure necessary to obtain the surrogate models was implemented by the software "UQLab: The Framework for Uncertainty Quantification" [26].

At last, to validate the surrogate models, a technique based on the leave-one-out cross-validation (LOO-CV), already tested on previous works [13, 14], was implemented. The LOO-CV technique allows to find a trade-off between the two objectives of minimizing the number N of simulations conducted with deterministic dosimetry and achieving an acceptable error. This technique consists in using all the deterministic simulations except one to obtain the surrogate model and predicting the value of the excluded simulation by using the model. Then the result obtained with stochastic dosimetry is compared with the one obtained with determinist dosimetry to compute the error.

The procedure is repeated recursively for each deterministic simulation. At last, summing all the errors of the leave one out process, the final error formula is:

$$\varepsilon_{LOO} = \frac{1}{N}\left[\frac{\sum_{i=1}^{N}\left(M(x_i)-\widehat{M}_{(-i)}^{PCK}(x_i)\right)^2}{Var[Y]}\right], \quad (3)$$

where N is the number of deterministic simulations, $M(x_i)$ is the result in x_i obtained with deterministic dosimetry, $\widehat{M}_{(-i)}^{PCK}(x_i)$ is the result of kriging metamodel in x_i obtained using all the outputs of the experimental design except x_i, and $Var[Y]$ is the output data variance obtained with deterministic dosimetry. We found that a number N = 60 simulations was sufficient to obtain an acceptable error.

C. Analysis of the Exposure

The surrogate models were built for the SAR mediated on whole tissue (namely, for the whole body, the whole head and the whole brain) and for the maximum SAR mediated on 10g in specific tissues (namely, for the skin, for the brain gray matter and for the cerebellum). After the validation of the surrogate models, it was possible to estimate the exposure levels for 1000 different combinations of the two input angles in the azimuth and elevation planes, with really low computational costs. Furthermore, for better characterizing the exposure assessment, on each SAR distribution an analysis of the percentage of values higher that the 70% of the maximum one was conducted and the Quartile Dispersion Coefficient (QDC) was calculated as:

$$QDC = \frac{Q_3-Q_1}{Q_3+Q_1}, \quad (4)$$

where Q_1 and Q_3 represent the first and third quartiles of the SAR distributions.

At last, the Sobol variance-based method was applied to perform a global sensitivity analysis, in order to evaluate which scan angle, between H-plane and E-plane, influences more the exposure. This technique consists in decomposing the variance of the results as the sum of the partial variances of contributions for each input parameter. The Sobol indices here reported are normalized and calculated as the ratios between the partial variances and the total variance of the system output [27].

III. Results

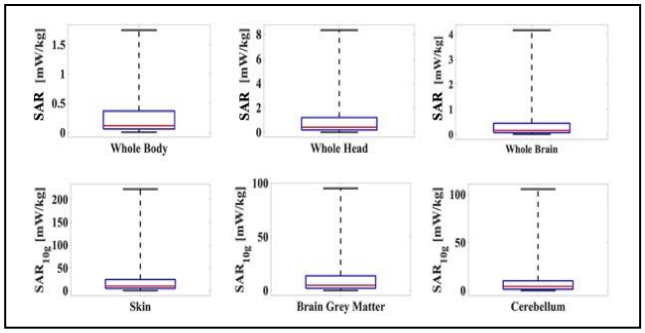

Figure 2. In the first row, the boxplots of the averaged SAR for the whole body, for the whole head and for the whole brain for 1000 different combinations of different two input scan angles. In the second row, the boxplots of the SAR mediated on 10 g for the skin, for the brain grey matter and for the cerebellum for the same 1000 different combinations of the two input scan angles. The lower and upper bound of the boxes represent the first and the third quartiles, the line is the median value, and the whiskers are the minimum and maximum values.

In Figure 2 there are illustrated the boxplots of the SAR average on whole body, whole head and whole brain, in the first row, and the boxplots of the SAR average on 10g for the skin, for the brain grey matter and for the cerebellum, in the second row, taking account 1000 possible different beamforming patters of the antenna. The boxplots report the median, the maximum and the minimum values and the first and the third quartiles of the distributions. As it can be noticed, the highest values of exposure were obtained in the case of the SAR average on mass for the head tissue, with a maximum of 8.35 mW/kg, a median of 0.42 mW/kg and a mean value of 1.23 mW/kg, whereas in the case of the SAR average on 10 g for the skin tissue, with a maximum of 222.23 mW/kg, a median of 9.71 mW/kg and a mean of 26.80 mW/kg. The reason of this behavior could be found considering the reciprocal position between the antenna and the Roberta model. The model head is indeed hit with higher probability by the *broadside* beam of the antenna (that is the beam with direction orthogonal to the array and providing the highest power), while this don't happen for the body lower part. Additionally, the skin is the most superficial tissue, so the majority of the radiation is absorbed by this tissue, providing the highest exposure levels in terms of SAR. It is important to underline that, anyway, all the values were well below the limits indicated by the ICNIRP guidelines [15].

Moreover, the analysis on the probability that a value is higher that the 70% of the maximum one highlighted very small percentages, i.e. a maximum of 7.2 % for the whole-body and a minimum of 2.8% in the cerebellum. This confirms that only when the broadside beam is directed towards Roberta model high exposure levels are experienced, whereas the beamforming patterns focused in other directions cause rapidly a decrease of SAR values.

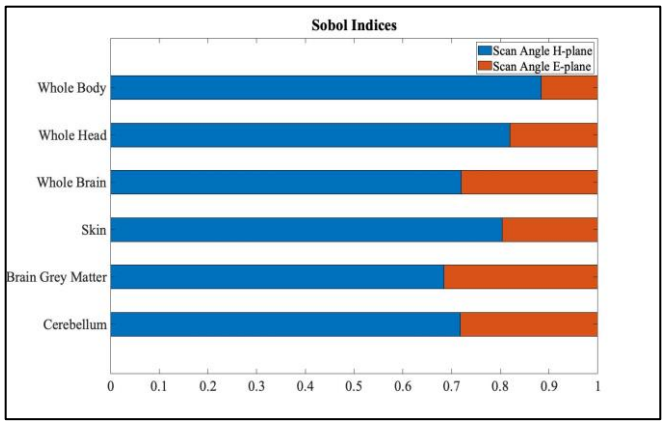

Figure 3. Sobol Indices of the SAR distributions.

Concerning the analysis on the QDC values, we found that the exposure scenario is characterized by a high variability, with QDC values raging from a minimum of 67% in the skin to a maximum of 76% in the cerebellum.

Finally, Figure 3 reports the results of the Sobol analysis. The figure shows that the scan angle in the H-plane influences the most the exposure levels, although also the scan angle in the E-plane is relevant, in particular for the tissues of the brain.

A deeper investigation of the obtained results can be found in [28].

IV. CONCLUSION

The work allowed to expand the knowledge on the RF-EMF human exposure, considering some of the novelties introduced by 5G indoor networks. The validity and the effectiveness of PC-Kriging technique was proven for the first time in assessing the human exposure levels in a highly variable scenario, considering the beamforming capability of a 5G AP antenna. Coupling deterministic dosimetry with different stochastic dosimetry techniques seems more and more a promising tool for dealing with the increase in variability and heterogeneity that the exposure scenarios encounter in real world.

ACKNOWLEDGMENT

The authors wish to thank ZMT Zurich MedTech AG (www.zmt.swiss) for having provided the simulation software SIM4Life.

REFERENCES

[1] J.G. Andrews, S. Buzzi, W. Choi, S.V. Hanly, A. Lozano, A.C. Soong, J.C. Zhang, "What will 5G be?," in *IEEE J. Sel. Areas Commun.* 2014, *32*, 1065–1082.

[2] E.G. Larsson, O. Edfors, F. Tufvesson, T.L. Marzetta, "Massive MIMO for next generation wireless systems," in *IEEE Commun. Mag.* 2014, *52*, 186–195.

[3] W.H. Chin, Z. Fan, R. Haines, "Emerging technologies and research challenges for 5G wireless networks," in *IEEE Wirel. Commun.* 2014, *21*, 106–112.

[4] S.M. Razavizadeh, M. Ahn, I. Lee, "Three-dimensional beamforming: A new enabling technology for 5G wireless networks," in *IEEE Signal Process. Mag.* 2014, *31*, 94–101.

[5] Recommendation ITU-T K Suppl.9 "5G technology and human exposure to RF EMF", 2017. 11.1002/1000/13473

[6] J.T. Bushberg, C.K. Chou, K.R. Foster, R. Kavet, D.P. Maxson, R.A. Tell, M.C. Ziskin, "IEEE Committee on Man and Radiation—COMAR Technical Information Statement: Health and safety issues concerning exposure of the general public to electromagnetic energy from 5G wireless communications networks," in *Health Physics*. 2020 Aug;119(2):236.

[7] C. Li, C. Xu, R. Wang, L. Yang, T. Wu, "Numerical evaluation of human exposure to 3.5-GHz electromagnetic field by considering the 3GPP-like channel features," in *Ann. Telecommun.* 2019, *74*, 25–33.

[8] D. Colombi, B. Thors, C. Törnevik, Q. Balzano, "RF energy absorption by biological tissues in close proximity to millimeter-wave 5G wireless equipment," in *IEEE Access* 2018, *6*, 4974–4981.

[9] B. Thors, D. Colombi, Z. Ying, T. Bolin, C. Törnevik, "Exposure to RF EMF from array antennas in 5G mobile communication equipment," in *IEEE Access* 2016, *4*, 7469–7478.

[10] S. Shikhantsov, A. Thielens, G. Vermeeren, P. Demeester, L. Martens, G. Torfs, W. Joseph, "Statistical approach for human electromagnetic exposure assessment in future wireless atto-cell networks," in *Radiat. Prot. Dosim.* 2019, *183*, 326–331.

[11] S. Shikhantsov, A. Thielens, G. Vermeeren, E.Tanghe, P. Demeester, L. Martens, G. Torfs, W. Joseph, "Hybrid ray-tracing/FDTD method for human exposure evaluation of a massive MIMO technology in an industrial indoor environment," in *IEEE Access* 2019, *7*, 21020–21031.

[12] P. Baracca, A. Weber, T. Wild, C.A. Grangeat, "statistical approach for RF exposure compliance boundary assessment in massive MIMO systems". In *Proceedings of the WSA 2018: 22nd International ITG Workshop on Smart Antennas*, Bochum, Germany, 14–16 March *2018*; pp. 1–6.

[13] E. Chiaramello, S. Fiocchi, M. Parazzini, P. Ravazzani, J. Wiart, "Stochastic Dosimetry for Radio-Frequency Exposure Assessment in Realistic Scenarios," In *Uncertainty Modeling for Engineering Applications,* Springer: Cham, Switzerland, 2019; pp. 89–102.

[14] M. Bonato, E. Chiaramello, S. Fiocchi, G. Tognola, P. Ravazzani, M. Parazzini, "Influence of low frequency Near-Field Sources Position on the Assessment of Children Exposure Variability using Stochastic Dosimetry," in *IEEE J. Electromagn. Rf Microw. Med. Biol.* 2019, *4*, 179–186.

[15] International Commission on Non-Ionizing Radiation Protection. Guidelines for limiting exposure to Electromagnetic Fields (100 kHz to 300 GHz), *Health Phys.* 2020, *118*, 483–524.

[16] 3GPP TR 38.802. Technical Specification Group Radio Access Network; Study on New Radio Access Technology Physical Layer Aspects (Release 14) v. 14.2.0, September 2017. Available online: http://www.3gorg (accessed on 15-02-2021).

[17] T. Uusitupa, I. Laakso, S. Ilvonen, K. Nikoskinen, "SAR variation study from 300 to 5000 MHz for 15 voxel models including different postures," in *Phys. Med. Biol.* 2010, *55*, 1157.

[18] M. Bonato, L. Dossi, E. Chiaramello, S. Fiocchi, S. Gallucci, G. Tognola, P. Ravazzani, M. Parazzini, "Human RF-EMF Exposure Assessment due to Access Point in Incoming 5G Indoor Scenario," in *IEEE J. Electromagn. Rf Microw. Med. Biol.* 2020, doi:10.1109/JERM.2020.3042696.

[19] G. Blatman, Adaptive Sparse Polynomial Chaos Expansions for Uncertainty Propagation and Sensitivity Analysis. Doctoral Dissertation, Université Blaise Pascal, Clermont-Ferrand, France, 2009.

[20] C. Gabriel, S. Gabriel, Y.E. Corthout, "The dielectric properties of biological tissues: I. Literature survey," in *Phys. Med. Biol.* 1996, *41*, 2231.

[21] S. Gabriel, R.W. Lau, C. Gabriel, "The dielectric properties of biological tissues: II. Measurements in the frequency range 10 Hz to 20 GHz," in *Phys. Med. Biol.* 1996, *41*, 2251.

[22] R. Schobi, B. Sudret, J. Wiart, "Polynomial-chaos-based Kriging," in *Int. J. Uncertain. Quantif.* 2015, *5*, 171–193.

[23] P. Kersaudy, B. Sudret, N. Varsier, O. Picon, J. Wiart, "A new surrogate modeling technique combining Kriging and polynomial chaos expansions–Application to uncertainty analysis in computational dosimetry," in *J. Comput. Phys.* **2015**, *286*, 103–117.

[24] B. Efron, T. Hastie, I. Johnstone, R. Tibshirani, "Least angle regression," in *Ann. Stat.* 2004, *32*, 407–499.

[25] C. Lataniotis, D. Wicaksono, S. Marelli, B. Sudret, *"UQLab User Manual—Kriging (Gaussian Process Modeling), Report # UQLab-V1.3-105, Chair of Risk, Safety and Uncertainty Quantification"*; ETH: Zurich, Switzerland, 2019.

[26] S. Marelli, B. Sudret, "UQLab: A framework for uncertainty quantification in Matlab," In Proc. 2nd Int. Conf. Vulnerability Risk Anal.Management, ICVRAM, and 6th Int. Symp. Uncertainty Modeling Anal., 2015, pp. 2554–2563.

[27] I.M. Sobol, "Global sensitivity indices for nonlinear mathematical models and their Monte Carlo estimates," in *Math. Comput. Simul.* 2001, *55*, 271–280.

[28] M. Bonato, L. Dossi, E. Chiaramello, S. Fiocchi, G. Tognola, M. Parazzini, "Stochastic Dosimetry Assessment of the Human RF-EMF Exposure to 3D Beamforming Antennas in indoor 5G Networks," in *Applied Sciences*. 2021 Jan;11(4):1751.